INVENTORY OF SUPPLEMENTAL INFORMATION

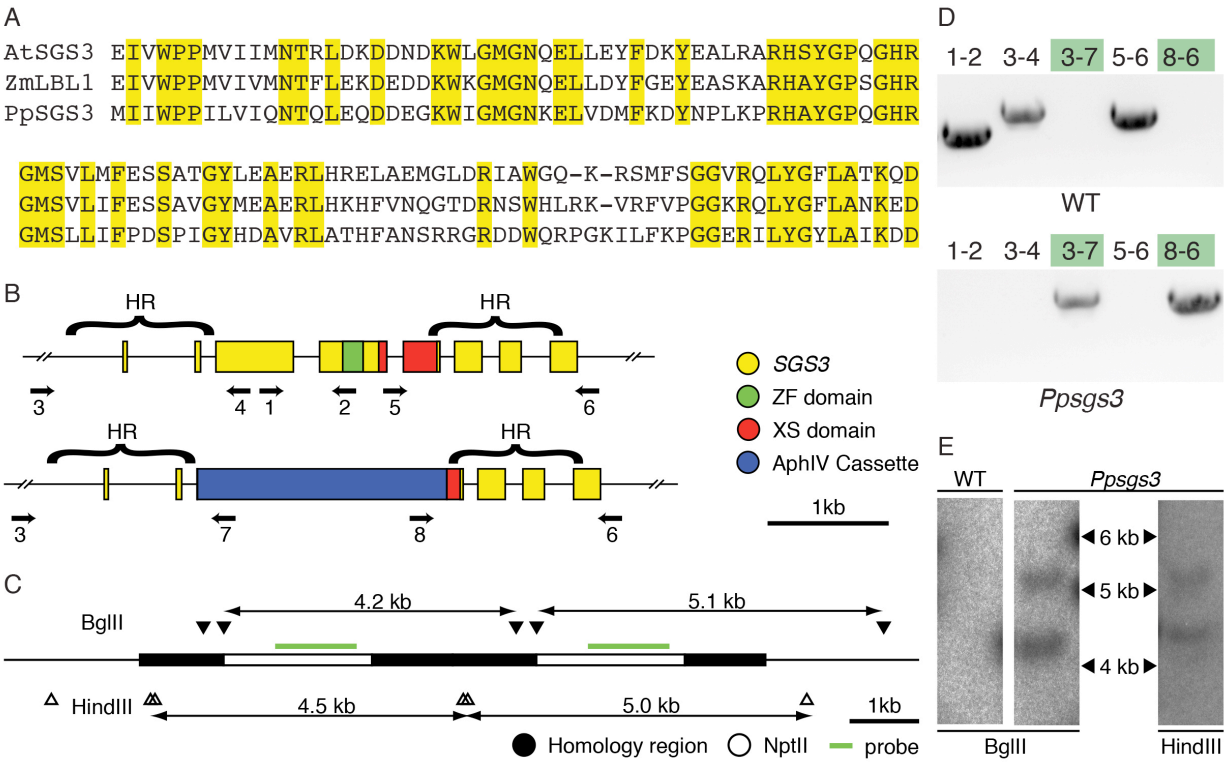

Figure S1, related to Figure 1. Construction of *Ppsgs3* mutants. (A) Alignment of XS domains of SGS3 homologs from *A. thaliana*, maize, and *P. patens*. Identical amino acids are highlighted in yellow. In the defining XS domain, PpSGS3 shares 67% sequence identity with AtSGS3 and 69.6% with LBL1. (B) Diagrammatic representations of the wild type (top) and mutant (bottom) *PpSGS3* loci. HR, homology regions for targeted recombination; arrows, positions of primers used in (D). (C) Diagram of the tandemly inserted cassette in *Ppsgs3.20*. Homology regions are shown in black, *AphIV* resistance cassette in white, probe in green. Arrowheads represent restriction sites for *Bgl*II (black) and *Hind*III (white). (D) PCR tests confirming targeted transgene insertions in *Ppsgs3*. Green highlighting, primer pairs with a product expected only for targeted recombination events. (E) Southern blot analysis of the *Ppsgs3.20* line, revealing a tandem insertion of the transformation cassette at the expected recombination site. Additional lines used in the study were validated by qPCR, and contain a single copy insertion.

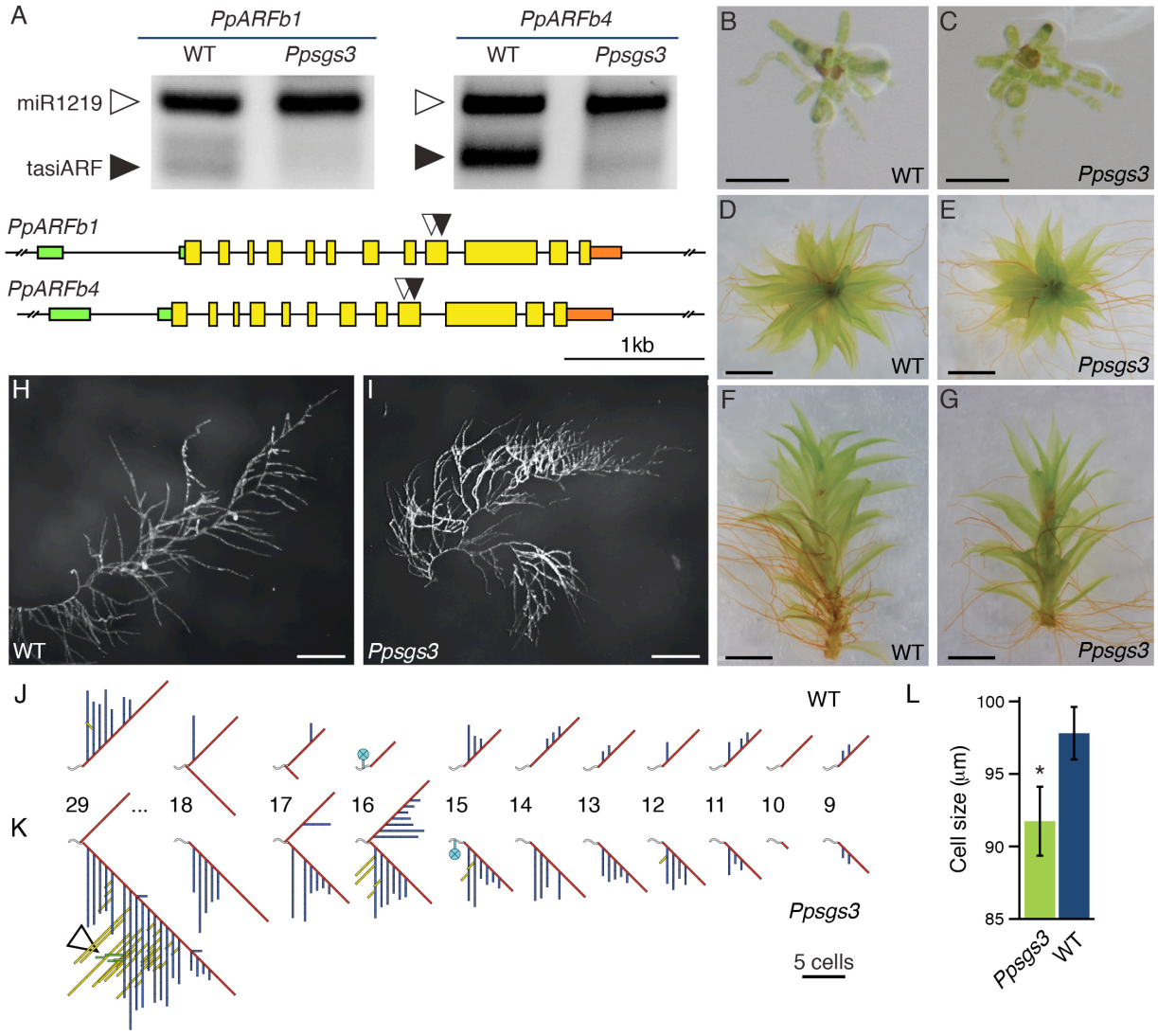

Figure S2, related to Figure 1. Altered tasiARF-directed *PpARFb4* transcript cleavage in *Ppsgs3* leads to increased protonemal branching. (A) RLM 5' RACE demonstrates a loss of tasiRNA-dependent cleavage (black arrow) of *PpARFb1* and *PpARFb4* transcripts in *Ppsgs3*, whereas cleavage at the miR1219 target site is unaffected (white arrow). Diagrams show the positions of small RNA-complementary sites in *PpARFb1* and *PpARFb4*. Green, 5' UTR; yellow, coding region; orange, 3' UTR. (B-C) Five day-old germinated spores of wild type (B) and *Ppsgs3* (C) shows that *Ppsgs3* spores are viable. Scale bar, 0.1 mm. (D-G) Gametophores from wild type (D, F) and *Ppsgs3* (E, G) plants grown for 1 month on BCD media are morphologically indistinguishable. Scale bar, 1mm. (H-K) Representative primary filaments from 3 week-old wild type (H, J) and *Ppsgs3* (I, K) plants shows a loss of branch determinacy in *Ppsgs3*.

Diagrams in J and K show branching patterns at cells 9-18 and at cell 29 measured from the tip of the primary filaments shown in H and I, respectively. Wavy lines, cells of the main filament; numbers, cell position relative to the filament tip; red lines, primary branches; blue lines, secondary branches; yellow lines, tertiary branches; green lines, quarternary branches (white arrowhead); cyan circles, gametophore buds. Branch lengths are proportional to the number of cells in the branch. Scale bar, 0.5 mm. Wild type protonemal branching largely follows a stereotyped pattern and is effectively determinate, with primary filaments extending from the center of the plant to its periphery producing one or occasionally two branches at nearly every cell. A subset of cells along these primary branches form secondary branches, but tertiary branches are rarely observed. In contrast, *Ppsgs3* protonemal filaments consistently show higher order branching patterns. Both the number of secondary branches and their length, measured as the number of cells per branch, are variably increased in *Ppsgs3*. Likewise, the number and length of tertiary branches is increased, and quaternary branches regularly occur near the base of *Ppsgs3* primary filaments. (L) Chloronemal cells in *Ppsgs3* are reduced in length by approximately 6% compared to wild type. Values (mean ± SE) were obtained from at least 8 filaments from 3 or more plants per genotype. *$P < 0.05$, Student's *t* test.

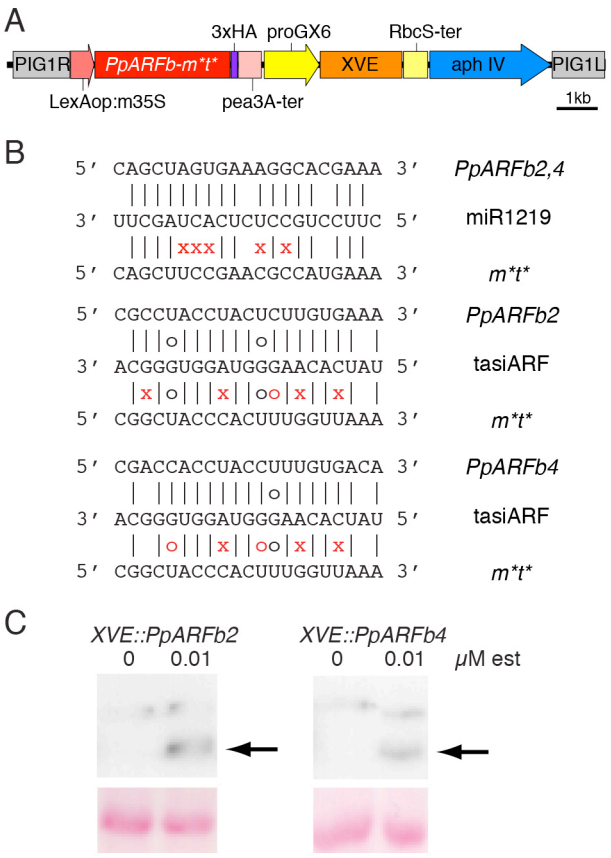

Figure S3, related to Figure 3**.** Construction of lines driving the estradiol-inducible expression of miR1219- and tasiARF-insensitive, HA-tagged variants of *PpARFb2* or *PpARFb4*. (A) Schematic representation of the constructs used to drive the estradiol-inducible expression of miR1219- and tasiARF-insensitive, HA-tagged variants of *PpARFb2* or *PpARFb4* (see Kubo *et al*. (2014) for more details). (B) Alignments of miR1219 and tasiARF to the *PpARFb2* and *PpARFb4* transcripts, illustrating the specific target site mutations introduced in the *m*t** overexpression variants to make their transcripts small RNA resistant. (C) Western blots incubated with anti-HA antibody show PpARFb2-HA and PpARFb4-HA (arrows) accumulate specifically in response to estradiol treatment.

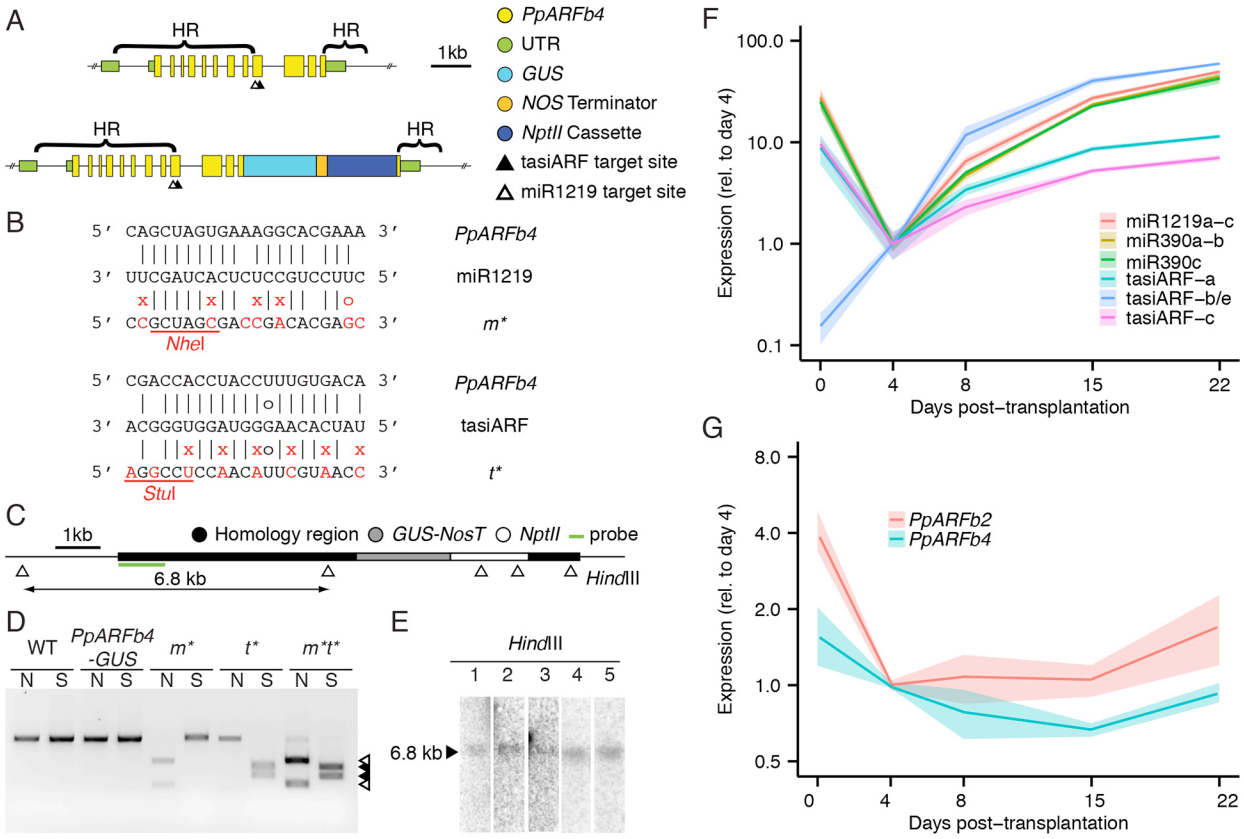

Figure S4, related to Figure 2. Developmental regulation of miR1219, tasiARF, and their *PpARFb* targets. (A-E) Construction of *PpARFb4-GUS* and its small RNA-resistant derivatives. (A) The *PpARFb4-GUS* lines were created by integration of a cassette containing the *GUS* reporter, *NOS* terminator, and *NptII* resistance marker directly upstream of the stop codon of *PpARFb4*. (B) miR1219- (*m**), tasiARF- (*t**), and miR1219- + tasiARF-insensitive (*m*t**) derivative strains for *PpARFb4-GUS* were created using a similar approach except that the 5' homology region contained a mutant version of the respective small RNA target site. Mutant small RNA target sites are distinguishable from wild type by the presence of a *Nhe*I or *Stu*I restriction site. (C) Diagram of the *PpARFb4-GUS* locus showing the positions of *Hind*III restriction sites (arrowheads). (D) Strains in which the miR1219- and/or the tasiARF-complementary site are mutated were validated by restriction digest: N, *Nhe*I; S, *Stu*I. Representative genotyping for four of the strains reported is shown. White arrowheads, restriction fragments expected for mutation of the miR1219 target site; black arrows, restriction fragments expected for mutation of the tasiARF target site. (E) Southern blots hybridized with the 5' homology region shows single targeted integrations into representative lines for wild type

(1), *PpARFb4-GUS* (2), *PpARFb4-GUS-m** (3), *PpARFb4-GUS-t** (4), and *PpARFb4-GUS-m*t** (5). Additional lines used in the study were validated by qPCR, and contain a single copy insertion. (F, G) In contrast to their *PpARFb* targets, expression levels of miR1219 and tasiARF increase substantially with plant age. (F) Expression levels (mean ± SE; $n \geq 3$) of miR390, miR1219, and tasiARF increases dramatically between day 4 and day 22 post-transplantation. Note the difference in expression levels for all small RNAs between protonema grown on cellophane-overlaid (0 days) versus regular (4 days) media. Except for tasiARF-c levels on day 8, all small RNA levels are significantly changed from that on day 4. (G) Expression levels (mean ± SE; $n \geq 3$) of *PpARFb2* and *PpARFb4* over the same time course change more subtly than observed for tasiARF and miR1219, and only *PpARFb4* levels at day 15 are significantly lower than on day 4. Note also here the difference in expression level between protonema grown on cellophane-overlaid (0 days) versus regular (4 days) media. Expression values are normalized to U6 (F) and *GAPDH* (G), and shown relative to expression levels at day 4. N.B.: Because growth conditions on cellophane plates substantially impacts gene expression levels, all additional expression was assayed in intact plants grown under the same conditions used for phenotypic analysis.

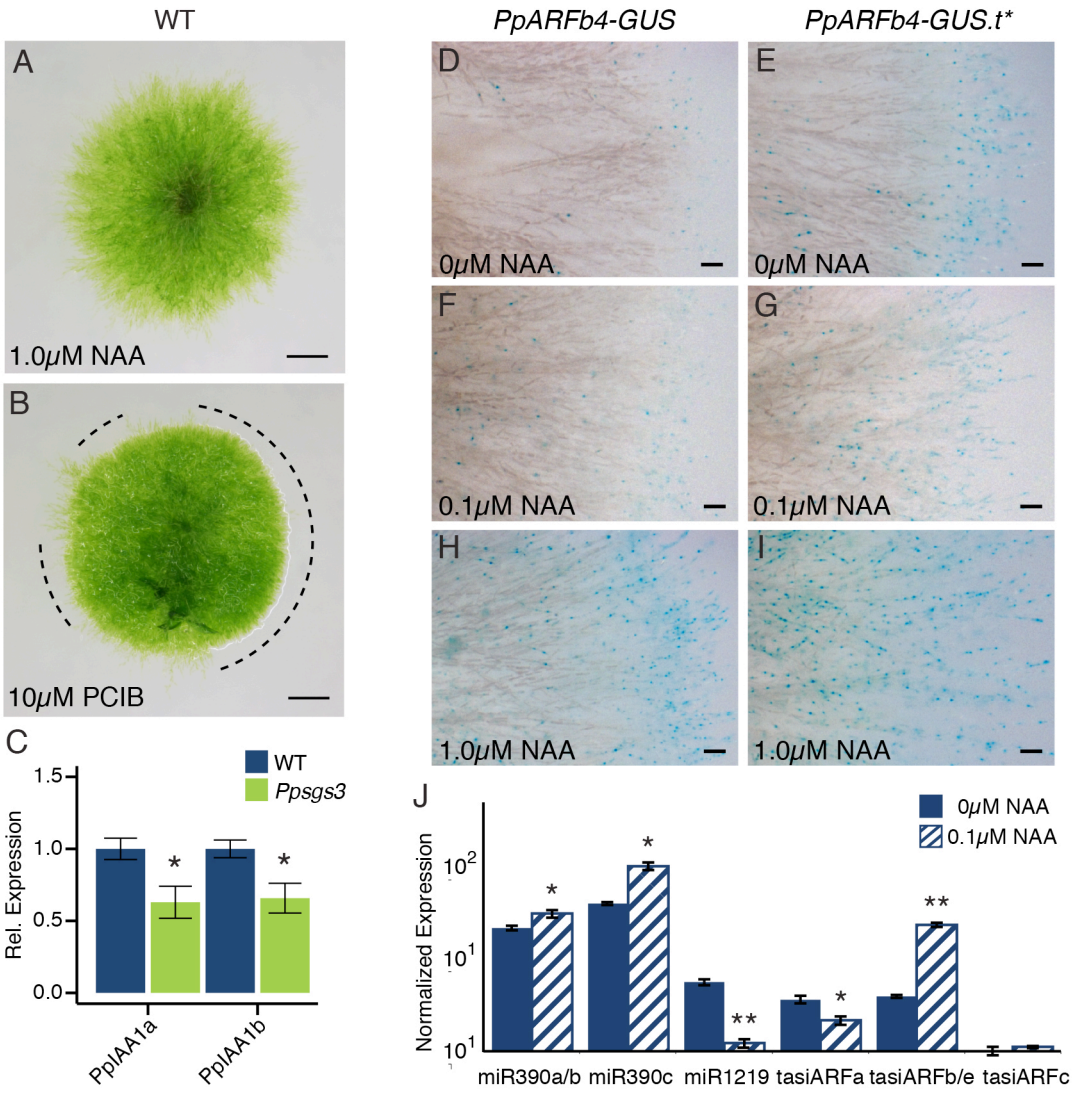

Figure S5, related to Figure 4. tasiARF regulation and auxin signaling converge to modulate expression of *PpARFb* repressor ARFs. (A-C) *Ppsgs3* mimics phenotypes resulting from the treatment of *Physcomitrella* with the 'anti-auxin' compound PCIB. (A) 15 day-old wild type plants grown on media containing 1 μM NAA develop an increased number of caulonemal filaments such that the protonemal network has a sparse appearance. (B) By contrast, plants grown in the presence of 10 μM PCIB develop few caulonemal filaments and a dense chloronemal network. Dotted lines denote regions of chloronemal filaments at the protonemal edge. Scale bar, 1 mm. (C) Expression levels (mean ± SE; n ≥ 3) of the auxin responsive genes *PpIAA1a* and *PpIAA1b* are lower in 15 day-old *Ppsgs3* as compared to wild type plants. *P < 0.05, Student's *t* test. Data presented is the same as the 0 μM NAA data point shown in **Figure**

5B, C. (D-J) Feedback regulation from auxin signaling on repressor *PpARFb* expression. (D-I) Representative GUS activity patterns for *PpARFb4-GUS* (D, F, H) and *PpARFb4-GUS-t** (E, G, I) plants grown on 0, 0.1, and 1μM NAA show that treatment with auxin leads to both an increase in reporter activity and an expansion of the PpARFb4-GUS expression domain. Scale bars = 0.1 mm. (J) Accumulation levels (mean ± SE; $n \geq 3$) of miR390, miR1219, and tasiARF in 15 day-old plants grown on 0 or 0.1 μM NAA show that the level of some small RNAs increases upon auxin treatment, whereas expression of others decreases. Small RNA levels are normalized to U6 RNA levels. * $P < 0.05$, ** $P < 0.01$, Student's *t* test.

SUPPLEMENTARY EXPERIMENTAL PROCEDURES

Plant growth

Unless otherwise indicated, the Gransden strain of *Physcomitrella patens* was cultured as described previously (Cove et al., 2009a) under continuous light at 25°C on BC media containing 5mM diammonium tartrate and 10 mM KNO_3 at pH 5.8 (aka BCDAT), supplemented with 0.9 μM FeSO4. Sporophyte development was induced on BC media containing 0.5 mM KNO_3 and 0.9 μM FeSO4. Subcultures were made by vortexing protonemal tissue in water with a glass bead for approximately one minute. Homogenized protonema was than plated onto solid media overlaid with cellophane discs (AA Packaging) and grown for 5-7 days. For phenotypic analyses, protonema was subcultured 2-5 times, and plantlets 1-3 mm in diameter transplanted to solid media without cellophane 5 days after the final subculture. Plant age is reported as the number of days after transplantation. For growth of protonema from spores, spores were sterilized as described (Cove et al., 2009a), suspended in water, and kept at 4°C in the dark for ~ 1 week, before being plated onto media. Chemical treatments were performed by adding NAA, PCIB, or beta-estradiol to media at the indicated concentrations. For growth on soil, cellophane-cultured plantlets were transplanted 5-7 days post-subculture to moist Rediearth (Sungro) and grown under a plastic dome for two months at 22°C under a 16/8 light/dark regime.

Cloning of transformation constructs

To create the *Ppsgs3* mutants, 5' and 3' homology regions were PCR-amplified from genomic DNA using Phusion DNA polymerase (NEB) and primer pairs EP23 + EP24B and EP27E + EP28E, respectively. PCR products were cloned into pCRII-TOPO (Invitrogen). Appropriate clones were digested using BglII + NotI (5' homology region) and KpnI + XbaI (3' homology region), and cloned between the BamHI + NotI and KpnI + XbaI sites of the BHSNR vector (Menand et al., 2007). The *PpARFb4-GUS* transformation vector was constructed using overlap extension PCR (Higuchi et al., 1988) from the following DNA segments amplified using Phusion DNA polymerase: the 5' *PpARFb4* homology region, amplified from *Physcomitrella* genomic DNA using primers EP196 + EP81, and subsequently using primers EP196 + EP376 to add the necessary overlap region; the 3' *PpARFb4* homology region, amplified using primers EP197 + EP199; the *GUS* reporter gene and 35S terminator, amplified using EP378 + EP379 from the

pKGWFS7 vector (Karimi et al., 2002); fragments of the pCR8 vector backbone (Invitrogen), amplified using EP273 + EP179 and EP180 + EP276, and the NptII resistance cassette, amplified from the BNRF vector (Menand et al., 2007) using EP377 + EP198. The fully assembled linear construct was treated with Polynucleotide Kinase (NEB) and self-ligated using the Rapid DNA Ligation Kit (Roche). To create mutations in the miR1219 target site (*m**), two segments of the *PpARFb4-GUS* construct were amplified using primer pairs EP273 + EP207 and EP206 + EP276, and the vector reassembled by overlap extension PCR and self-ligation as described above. Mutations in the tasiARF target site (*t**) were created similarly except that segments of the *PpARFb4-GUS* construct were amplified with EP273 + EP209 and EP208 + EP276. To create the estradiol-inducible ARFb overexpression constructs, cDNA clones of *PpARFb2* and *PpARFb4* were mutated at the miR1219 and tasiARF target sites as indicated, and inserted into vector pPGX6 (Kubo et al., 2013) with homology to allow insertion into the neutral PIG1 locus in the *Physcomitrella* genome.

***Physcomitrella* transformation**

Protoplast transformations were carried out using 10-30 µg linearized DNA as described previously (Cove et al., 2009b) with the following minor adjustments. For protoplast isolation, protoplasts were digested for 30 minutes in 2% Driselase (Sigma-Aldrich), followed by one round of filtering using 40 mm Cell Strainers (BD Falcon). Washes were performed using 8% D-mannitol without CaCl2, and post-transformation dilution in D-mannitol was performed over the course of 30 mins. *Ppsgs3* transformants were screened using primer pairs EP119 + EP120, EP123 + EP124, and EP122 + EP61I to test for the presence of the wild type locus, and primers EP119 + EP126 and EP61I + EP121 to test for the targeted 5' and 3' transgene insertion, respectively. Transformants for *PpARFb4-GUS* and the different small RNA resistant derivatives were tested for a targeted 5' transgene insertion using EP128 + EP70. To verify the presence of the miR1219 and tasiARF target site mutations, the region containing these sites was amplified with EP91F + EP210 and digested with NheI and StuI to test for the *m** and *t** mutations, respectively. Transformants were further analyzed by Southern blot as described (Hiwatashi et al., 2001), or by qPCR (Fletcher, 2014). *Ppsg3* blots were hybridized with a probe amplified from the hygromycin resistance gene using EP61H + EP125. For *PpARFb4-GUS* and its small RNA resistant derivatives, blots were hybridized with a probe amplified from the 5' homology

region using EP354 + EP64B.R. To assay transgene copy number by qPCR, DNA from wild type and the individual *Ppsgs3* strains was amplified using EP502 + EP431 and EP505 + EP506 to assess the relative abundance of the 5' homology region and a genomic control region, respectively. In the case of *PpARFb4-GUS* and its small RNA-resistant derivatives, primers GUS.F + GUS.R were used instead. Transgene copy number was calculated using the formula:

$$\frac{2^{(C_t \text{ control primers, norm. strain} - C_t \text{ transgene primers, norm. strain})}}{2^{(C_t \text{ control primers, test strain} - C_t \text{ transgene primers, test strain})}}$$

Only transformants with a single site of insertion were analyzed further, but for each genotype, lines derived from multiple such transformants were characterized.

Phenotypic analyses

Plants constituting a single biological replicate were grown simultaneously on the same batch of plates with mutants and wild type controls paired on each plate. All phenotypic observations were performed on at least two independent lines for each genotype, and were found to be consistent across independent lines. Gametophores were counted by visually examining plants using a dissecting microscope. Only buds with at least one phyllid were counted. Each data point represents the mean ± SE of 10 or more plants, and the same plants were followed over the time course presented. Branching was analyzed on 3 week-old plants fixed in FAA (3.7% formaldehyde, 5% acetic acid, 50% ethanol). Individual filaments were isolated and inspected under a dissecting microscope to note every protonemal cell, gametophore bud, and branch position. For cell measurements, protonema were photographed on a compound microscope and the length (mean ± SE) of chloronemal cells 3 to 5 cells from the tip measured using ImageJ. Branch analysis and cell measurements were obtained from at least 8 filaments from 3 or more plants in each genotype. Significant effects on phenotype were tested using the Student's *t* test.

qRT-PCR analysis

Unless otherwise indicated, RNA was extracted from plants grown on media without cellophane. For this, forty 4 day-old, fifteen 8 day-old, or six 15 or 22 day-old plants were excised from the media and incubated with shaking for 5 minutes at room temperature in ~3 mL Buffer QG (Qiagen). This step was repeated and followed by two 10 minute-long washes with water. Tissue was then blotted dry and ground in liquid nitrogen. Total RNA was extracted using Trizol

reagent (Invitrogen) according to the manufacturer's suggested protocol. For extractions from protonema grown on cellophane-overlaid plates, protonema were cultured for 5 days, collected on a paper towel to blot dry, and frozen for RNA extraction as above. cDNA was synthesized with oligo(dT) primers using the Superscript III kit (Invitrogen) following the manufacturer's suggested protocol. qRT-PCR was performed on the CFX96 Real-Time PCR Detection System with iQ SYBR Green Supermix (BioRad). The specificity of all amplification products was determined using dissociation curve analyses. Relative quantification (RQ) values were calculated based on at least two technical and three biological replicates using the formula $2^{(C(t)GAPDH - C(t)gene)}$ to normalize gene expression levels to levels of *GAPDH*. Significant effects on expression values were tested using the Student's *t* test.

Small RNA analysis

Total RNA was extracted as above. Small RNA levels were determined by qPCR using a protocol modified from Varkonyi-Gasic et al. (Varkonyi-Gasic et al., 2007), in that distinct hairpin primers with variant loop sequences were designed for each unique small RNA to increase specificity. qRT-PCR was performed using IQ SYBR Green Supermix (Bio Rad). Small RNA expression levels normalized to U6 levels were calculated based on at least two technical and three biological replicates using the formula $2^{(C(t)U6 - C(t)sRNA)}$. Significant effects on small RNA levels were tested using the Student's *t* test. RLM 5' RACE was performed on RNA extracted from cellophane-grown tissue as described previously (Axtell et al., 2007).

Histochemical staining

Plants were excised from the media and incubated in staining solution containing 50 mM sodium phosphate (pH 7.0), 10 mM EDTA, 0.05% Triton-X, 2 mM ferrocyanide, 2 mM ferricyanide, 0.05% X-Gluc, 75 mg/L Kanomycin, and 150 mg/L Spectinomycin following vacuum-infiltration for ~45 minutes at ~600 mm Hg. Plants were incubated for 14 days at 37°C, exchanging staining solution every 3 days. Subsequently, plants were vacuum-infiltrated with FAA, cleared in 70% ethanol, and examined under a dissecting microscope. Periodicity in marker expression was assessed by counting the number of GUS positive cells in consecutive filaments along the edge of plants. Significant signatures of periodicity in the data were tested using the Ljung-Box test.

Primers

Primer	Sequence	Purpose	[1]Source Pub.
EP367	ATCTGCACGTGGGAACCAGCTTTGCT	5' RACE	Axtell *et al.* 2007
EP368	GGCTTGACGTTCCACGAGGTATTTCG	5' RACE	Axtell *et al.* 2007
EP369	CACTCGACACGTCGTTGCTGAGAGTT	5' RACE	Axtell *et al*. 2007
EP370	ATGAGGAGGTCCGGGAGGATTCGATA	5' RACE	Axtell *et al*. 2007
EP464	GTTGGCTCTGGTGCCCACGTGCTTCGATTCG CACCAGAGCCAACAAGCTA	cDNA synthesis: miR1219a-c	
EP453	GTTGGCTCTGGTGCAGGGTCCGAGGTATTC GCACCAGAGCCAACGGCGCT	cDNA synthesis: miR390a-c	
EP521	GTTGGCTCTGGTGCCCACGTGCTTCGATTCG CACCAGAGCCAACTGAAGC	cDNA synthesis: tasiAP2a	
EP522	GTTGGCTCTGGTGCTGCCGTCCACTGATTCG CACCAGAGCCAACGGAAGC	cDNA synthesis: tasiAP2b	
EP523	GTTGGCTCTGGTGCCACGCTGGAGCAATTC GCACCAGAGCCAACCTAAGC	cDNA synthesis: tasiAP2d	
EP524	GTTGGCTCTGGTGCGTGATGGCGAACATTC GCACCAGAGCCAACATAAGC	cDNA synthesis: tasiAP2f	
EP466	GTTGGCTCTGGTGCTGCCGTCCACTGATTCG CACCAGAGCCAACTGCCCA	cDNA synthesis: tasiARFa	
EP468	GTTGGCTCTGGTGCCACGCTGGAGCAATTC GCACCAGAGCCAACCAACCA	cDNA synthesis: tasiARFb/c/e	
EP180	ATGGTCATAGCTGTTTCCTGG	cloning	
EP196	AACGACGGCCAGTAGATCTCCGTTGTTGTTT GAGGACGTG	cloning	
EP197	CAGCTATGACCATAGATCTTCTGGTTTAGGG GACTACGG	cloning	
EP198	CTCGTCACAGTTGGGCGGCCGCGAATTCGA GCTCGG	cloning	
EP199	CGCGGCCGCCCAACTGTGACGAGGACGATG	cloning	
EP206	CCGCTAGCGACCGACACGAGCGGGTATCAC CATGGGAG	cloning	
EP207	GCTCGTGTCGGTCGCTAGCGGATTCGTCCCA CTCCACTTTC	cloning	
EP208	AGGCCTCCAACATTCGTAACCGACTCGTCC CCGCAG	cloning	
EP209	GGTTACGAATGTTGGAGGCCTGCGCTTTGG CCTAGGC	cloning	
EP377	GATTGTCGTTTCCCGCGTCGACATAACTTCG TATAATG	cloning	
EP378	GGAGGTGGAGGTGGAGCTGTCGACATGTTA CGTCCTGTAGAAACC	cloning	
EP379	CATTATACGAAGTTATGTCGACGCGGGAAA CGACAATC	cloning	
EP430	TTCTCCCGCAATATTCAAGC	cloning	
EP55E	GGTGCTTTTGTTCCAGTTCC	cloning	
EP81	AGCTCCACCTCCACCTCCGCCACTGCTCTGA ACTGC	cloning	
EP128	TTCGTAGGATGACAAACTGGAG	*PpARFb4-GUS* PCR test	

Primers continued

Primer	Sequence	Purpose	Source Pub.
EP170	TGATAGCGCGTGACAAAAAC	*PpARFb4-GUS* PCR test	
EP210	CCGTTGATTTGGGATACGTC	*PpARFb4-GUS* PCR test	
EP91F	CCGGCTGTATTCATGACTTTG	*PpARFb4-GUS* PCR test	
EP119	TCTTCCAAGTTCCGATCACC	*Ppsgs3* PCR test	
EP120	GGCTTTTTCCGTTCTTGTCTC	*Ppsgs3* PCR test	
EP121	GCTTCATGCTGTTGCTTTTG	*Ppsgs3* PCR test	
EP122	GCGCTTGATACAGTGGATTG	*Ppsgs3* PCR test	
EP123	AGGATCGAACAGGAACAACG	*Ppsgs3* PCR test	
EP124	GTACGCACCTTTCCTTCGTC	*Ppsgs3* PCR test	
EP126	ATGGAATCCGAGGAGGTTTC	*Ppsgs3* PCR test	
EP61I	GGTTTCGCTCATGTGTTGAG	*Ppsgs3* PCR test	
EP410	CCAACTTACGTGGTGGGAGT	qRT-PCR *GAPDH*	Prigge *et al.*, 2010
EP411	GATCCCAAACTTCTCGTCCA	qRT-PCR *GAPDH*	Prigge *et al.*, 2010
EP452	TGGATTAAGCTCAGGAGGGAT	qRT-PCR miR390a/b	
EP454	GTGCAGGGTCCGAGGT	qRT-PCR miR390a-c	
EP481	TGGATTGAGCTCAGGAGGGAT	qRT-PCR miR390c	
EP515	GTCTTTAGGGCAGGCGAGTGAGCAATC	qRT-PCR *PpAP2a*	Cho *et al.,* 2012
EP516	GTGTGGCATGCTGCAAACTATTGGGTG	qRT-PCR *PpAP2a*	Cho *et al.,* 2012
EP517	AAAGTACAGGCGTCTATAGCTGGTGC	qRT-PCR *PpAP2b*	Cho *et al.,* 2012
EP518	GGCTTATTTGAAACGGACCGCGAA	qRT-PCR *PpAP2b*	Cho *et al.,* 2012
EP519	GCAAGCAGTCTACTCATCATGCCA	qRT-PCR *PpAP2c*	Cho *et al.,* 2012
EP520	TTGATGCTGGCGGCTTTCAGCTTT	qRT-PCR *PpAP2c*	Cho *et al.,* 2012
EP375	AGCCAATTTGTTCGACTGGT	qRT-PCR *PpARFb2*	
EP373	GTGAAAGGCACGAAAGGGTA	qRT-PCR *PpARFb2*	
EP479	GTGATAGGCACGAAAGGGTT	qRT-PCR *PpARFb1*	
EP480	CCCTGCAGGACCTTAAACAG	qRT-PCR *PpARFb1*	
EP394	CCAACTTGTTGGACTGCTGA	qRT-PCR *PpARFb4*	
EP373	GTGAAAGGCACGAAAGGGTA	qRT-PCR *PpARFb4*	
EP398	ATCCGGGAGTCCGAGCTTC	qRT-PCR *PpIAA1a*	Prigge *et al.*, 2010
EP399	GGTTCTGCGCAGGAGGTG	qRT-PCR *PpIAA1a*	Prigge *et al.*, 2010
EP400	CGGTGGTCAGAATGGGTCA	qRT-PCR *PpIAA1b*	Prigge *et al.*, 2010
EP401	CCCACAGTCTGGTTCTGCG	qRT-PCR *PpIAA1b*	Prigge *et al.*, 2010
EP511	AGGTGAATTTGCACCAAAGC	qRT-PCR *PpIAA2*	
EP512	GCCAACCCACTGTCTGATTC	qRT-PCR *PpIAA2*	
EP418	CCATGCTGGAGAAGGCTATC	qRT-PCR *PpRSL1*	
EP419	TCGGTTTCTCTGACGACTCC	qRT-PCR *PpRSL1*	
EP531	GCAACCGATCCTCAGAGTGT	qRT-PCR *PpRSL5*	Pires *et al*. 2013
EP532	TCAACCTTGGCTCCATTAGG	qRT-PCR *PpRSL5*	Pires *et al*. 2013
EP533	AAATCTCGTGCCAAATGGAG	qRT-PCR *PpRSL6*	Pires *et al*. 2013
EP534	CATCCAGAACTCGTCGGATT	qRT-PCR *PpRSL6*	Pires *et al*. 2013

Primers continued

Primer	Sequence	Purpose	Source Pub.
EP565	GTGGAGATGATGCTCCCATT	qRT-PCR *PpZF*	
EP566	TCTCACAAATTCCAATTGCTTG	qRT-PCR *PpZF*	
EP525	TGGATTTAGGGTGTGATGAGT	qRT-PCR tasiAP2a/b/f	
EP526	TGGATTTGGGGTGTGATGACT	qRT-PCR tasiAP2d	
EP497	GTGCGTGATGGCGAAC	qRT-PCR tasiAP2f	
EP455	TGGATGTATCACAAGGGTAGG	qRT-PCR tasiARFa	
EP467	GTGCTGCCGTCCACTG	qRT-PCR tasiARFa/ tasiAP2b	
EP469	GTGCCACGCTGGAGCA	qRT-PCR tasiARFb/c/e	
EP462	TGGATTTGTCTCAAGGGTACG	qRT-PCR tasiARFb/e	
EP463	TGGATTTGTCTCAAGGGTAGC	qRT-PCR tasiARFc	
EP459	CGATACAGAGAAGATTAGCATGG	qRT-PCR *U6*	
EP460	GGACCATTTCTCGATTTGTG	qRT-PCR *U6*	
EP125	GGAACCCTAATTCCCTTATCTG	Southern Probe	
EP354	TGCATAAGCATGCGTGGTAG	Southern Probe	
EP61H	GACGGCAATTTCGATGATG	Southern Probe	
EP64B.R	TTTTTGTGGACCCTTCATCG	Southern Probe	
EP431	CGAATCCGCACCATAATTTC	Transgene qPCR	
EP502	GGTTTTGGTTGTTGCAGCTT	Transgene qPCR	
EP505	CAAGCTGGTGAAGGAGGAAG	Transgene qPCR	
EP506	ACACCAACAAACCCTTCTGC	Transgene qPCR	
GUS.F	CTGCGTTTCGATGCGGTCACTCATT	Transgene qPCR	
GUS.R	CATCACGCAGTTCAACGCTGACATC	Transgene qPCR	

[1]Axtell, M.J., Snyder, J.A., and Bartel, D.P. (2007). Common functions for diverse small RNAs of land plants. Plant Cell *19*, 1750-1769. Cho, S.H., Coruh, C., and Axtell, M.J. (2012). miR156 and miR390 regulate tasiRNA accumulation and developmental timing in *Physcomitrella patens*. Plant Cell *24,* 4837-4849. Pires, N.D., Yi, K., Breuninger, H., Catarino, B., Menand, B., and Dolan, L. (2013). Recruitment and remodeling of an ancient gene regulatory network during land plant evolution. Proc. Nat. Acad. Sci. *110*, 9571-9576. Prigge, M.J., Lavy, M., Ashton, N.W., and Estelle, M. (2010). *Physcomitrella patens* auxin-resistant mutants affect conserved elements of an auxin-signaling pathway. Current Biology *20*, 1907-1912.

SUPPLEMENTARY REFERENCES

Axtell, M.J., Snyder, J.A., and Bartel, D.P. (2007). Common functions for diverse small RNAs of land plants. Plant Cell *19*, 1750-1769.

Cove, D.J., Perroud, P.-F., Charron, A.J., McDaniel, S.F., Khandelwal, A., and Quatrano, R.S. (2009a). Culturing the moss *Physcomitrella patens*. Cold Spring Harb Protoc *2009*, pdb.prot5136.

Cove, D.J., Perroud, P.-F., Charron, A.J., McDaniel, S.F., Khandelwal, A., and Quatrano, R.S. (2009b). Transformation of the moss *Physcomitrella patens* using direct DNA uptake by protoplasts. Cold Spring Harb Protoc *2009*, pdb.prot5143.

Fletcher, S.J. (2014). qPCR for quantification of transgene expression and determination of transgene copy number. Methods Mol. Biol. *1145*, 213-237.

Higuchi, R., Krummel, B., and Saiki, R.K. (1988). A general method of in vitro preparation and specific mutagenesis of DNA fragments: study of protein and DNA interactions. Nucleic Acids Res *16*, 7351-7367.

Hiwatashi, Y., Nishiyama, T., Fujita, T., and Hasebe, M. (2001). Establishment of gene-trap and enhancer-trap systems in the moss *Physcomitrella patens*. Plant J *28*, 105-116.

Karimi, M., Inzé, D., and Depicker, A. (2002). GATEWAY vectors for *Agrobacterium*-mediated plant transformation. Trends Plant Sci *7*, 193-195.

Kubo, M., Imai, A., Nishiyama, T., Ishikawa, M., Sato, Y., Kurata, T., Hiwatashi, Y., Reski, R., and Hasebe, M. (2013). System for stable β-estradiol-inducible gene expression in the moss *Physcomitrella patens*. PLoS ONE *8*, e77356.

Menand, B., Yi, K., Jouannic, S., Hoffmann, L., Ryan, E., Linstead, P., Schaefer, D.G., and Dolan, L. (2007). An ancient mechanism controls the development of cells with a rooting function in land plants. Science *316*, 1477-1480.

Varkonyi-Gasic, E., Wu, R., Wood, M., Walton, E.F., and Hellens, R.P. (2007). Protocol: a highly sensitive RT-PCR method for detection and quantification of microRNAs. Plant Methods *3*, 12.